Chemistry & Biology
Article

Laboratory Evolution of High-Redox Potential Laccases

Diana Maté,[1] Carlos García-Burgos,[1] Eva García-Ruiz,[1,2] Antonio O. Ballesteros,[1] Susana Camarero,[1,2] and Miguel Alcalde[1,*]
[1]Department of Biocatalysis, Institute of Catalysis, CSIC, Cantoblanco, 28049 Madrid, Spain
[2]Centro de Investigaciones Biológicas, CSIC, 28040 Madrid, Spain
*Correspondence: malcalde@icp.csic.es
DOI 10.1016/j.chembiol.2010.07.010

SUMMARY

Thermostable laccases with a high-redox potential have been engineered through a strategy that combines directed evolution with rational approaches. The original laccase signal sequence was replaced by the α-factor prepro-leader, and the corresponding fusion gene was targeted for joint laboratory evolution with the aim of improving kinetics and secretion by *Saccharomyces cerevisiae*, while retaining high thermostability. After eight rounds of molecular evolution, the total laccase activity was enhanced 34,000-fold culminating in the OB-1 mutant as the last variant of the evolution process, a highly active and stable enzyme in terms of temperature, pH range, and organic cosolvents. Mutations in the hydrophobic core of the evolved α-factor prepro-leader enhanced functional expression, whereas some mutations in the mature protein improved its catalytic capacities by altering the interactions with the surrounding residues.

INTRODUCTION

Laccases (EC 1.10.3.2) belong to the group of blue multicopper oxidases along with ceruloplasmin, ascorbate oxidase, and bilirubin oxidase, among others. Laccase is one of the oldest enzymes reported and it is currently arousing great interest in the scientific community because of its very basic requirements (it just needs air to work and its only released by-product is water) and huge catalytic capabilities, making it one of the "greenest" enzymes of the 21st century (Rodgers et al., 2010; Riva, 2006; Alcalde et al., 2006a).

In a well-conserved and better fitting laccase scaffold, the characteristic paramagnetic blue copper at the T1 site is responsible for sequestering one electron from the reducing substrate and transferring it to the trinuclear T2/T3 copper cluster, where molecular oxygen binds (Solomon et al., 1996; Giardina et al., 2010). As a generalist biocatalyst, laccase is capable of oxidizing dozens of different compounds (phenols, polyphenols, benzenothiols, polyamines, hydroxyindols, aryl diamines, Mn^{2+}, and $Fe(EDTA)^{2-}$), and its substrate promiscuity can be even further expanded by the use of redox mediators (diffusible electron carriers from natural or synthetic sources) (Call and Mucke, 1997; Gianfreda et al., 1999; Kunamneni et al., 2008a; Cañas and Camarero, 2010). Laccases are commonly classified as low-medium and High Redox Potential Laccases (HRPLs) according to their redox potential at the T1 site (ranging from +430 mV in bacterial and plant laccases to +790 mV in some fungal laccases), and the latter are by far the most important from a biotechnological point of view (Rodgers et al., 2010; Alcalde, 2007). HRPLs are typically secreted by lignolytic basidiomycetes, the so-called white-rot fungi, displaying a high catalytic rate along with the capacity to oxidize compounds with higher redox potential that cannot be transformed by their medium and low redox potential laccase counterparts (Shleev et al., 2005a).

However, the engineering of HRPLs for practical uses has hardly been addressed because of the lack of suitable expression systems to improve them through directed evolution. Although *Escherichia coli* is the preferred host organism for in vitro evolution experiments, the differences between the eukaryotic expression system for HRPLs and that of bacteria (codon usage, missing chaperones, posttranslational modifications such as glycosylation, or the formation of disulfide bridges) are hurdles that are not easily overcome. Accordingly, all attempts to functionally express fungal laccases in bacteria have so far ended up in misfolding and the formation of inclusion bodies (Kunamneni et al., 2008b). However, the secretory machinery of *Saccharomyces cerevisiae* permits posttranslational modifications, and it is also an excellent host for performing laboratory evolution experiments (Alcalde, 2010). Indeed, the high level of homologous recombination enables scientists to produce in vivo shuffled mutant libraries or to develop new tools to generate diversity (Cherry et al., 1999; Okkels, 2004; Bulter et al., 2003; Alcalde et al., 2006b; Zumárraga et al., 2008a). In this context, we have already used directed evolution to improve the functional expression of the low redox potential laccase from the ascomycete *Myceliophthora thermophila* in *S. cerevisiae*, to confer organic cosolvent tolerance, as well as to perform semirational studies (Bulter et al., 2003; Zumárraga et al., 2007, 2008b). Unfortunately, the past success with this low redox potential laccase cannot be easily translated to its HRPL counterparts, since the differences between the basidiomycete processing mechanism of HRPLs and that of the ascomycete *S. cerevisiae* impair functional expression at the levels required for directed evolution, as can be deduced from recent studies (Festa et al., 2008; Cusano et al., 2009; Miele et al., 2010).

Here, for the first time we describe the directed evolution of a high redox potential laccase functionally expressed in *S. cerevisiae* enhancing its activity and thermostability. Our starting point was the basidiomycete PM1 HRPL, which exhibits

 ©2010 Elsevier Ltd All rights reserved

remarkable stability and activity, including thermal activation (Coll et al., 1993a). After replacing the native signal sequence with the α-factor prepro-leader to regulate heterologous protein trafficking, the fusion protein was subjected to eight rounds of laboratory evolution in combination with rational approaches. The last mutant in this process constitutes a valuable point of departure for further directed evolution experiments to tailor custom-made HRPLs with improved properties.

RESULTS AND DISCUSSION

Point of Departure for Evolution: The Construction of α-PM1

Our starting point was the HRPL from basidiomycete PM1 (CECT 2971). In addition to its high redox potential (above +700 mV), PM1 laccase is highly stable in the pH interval of 3 to 9 and at high temperature (with optimal thermoactivity at 80°C) (Coll et al., 1993a, 1993b). These features are highly desirable not only for practical use, but also to perform directed evolution experiments. Bearing in mind that the accumulation of beneficial mutations over several rounds of laboratory evolution generally destabilizes the protein scaffold, the better the stability of the starting enzyme, the greater the likelihood of achieving the desired improvements without jeopardizing the protein's function (Bloom and Arnold, 2009). In the first place, the PM1 cDNA with the native signal leader was cloned into the corresponding shuttle vector, although no detectable levels of functional expression were found in *S. cerevisiae*. To enhance its expression to values that can be detected in the screening assays, the PM1 native signal sequence was replaced by different leader peptides commonly used to express heterologous proteins in yeast (see Supplemental Experimental Procedures available online). The best result was obtained with the α-PM1 construction (Figure S1) constituted by the prepro-leader of the yeast α-factor mating pheromone (Shuster, 1991) coupled to the mature PM1, which gave rise to very low but detectable levels of expression (~35 mU/L). The coefficients of variance (CV) for the screening assays were adjusted throughout the evolution process (achieving CVs below 11% from the third cycle of evolution onward) and the microfermentation conditions were optimized (copper uptake, medium composition, oxygen availability, and temperature) (see Supplemental Experimental Procedures).

Laboratory Evolution of α-PM1

A directed evolution strategy was elaborated according to the following rules: (1) to better fulfill the requirements of the host's secretory pathway for functional laccase expression, the whole fusion gene was targeted for random mutagenesis and/or recombination, thereby jointly evolving both the α-factor prepro-leader and the foreign laccase gene to adjust both elements for successful exportation by *S. cerevisiae*; (2) to ensure the improvement in activity was not substrate dependent, screening assays based on the oxidation of phenolic (2,6 DMP) and non-phenolic (ABTS) compounds were validated and employed during the molecular evolution; (3) to guarantee the overall thermostability of the ultimate mutant, the drops in stability produced by the accumulation of mutations during evolution were detected and recovered by rational approaches coupled with the screening of mutant libraries for thermostability; and (4) mutations representing significant improvements during the first rounds of in vitro evolution but that were not eventually selected after recombination and screening, were recovered individually, analyzed, and introduced into the last variants by site-directed mutagenesis. In addition, new mutations identified in a parallel directed evolution experiment that we performed with other highly related HRPL (the laccase from *Pycnoporus cinnabarinus* with 77% identity to the PM1 laccase) were individually tested in the α-PM1 mutants.

The generation of diversity was emulated by taking advantage of the eukaryotic machinery of *S. cerevisiae*. From our previous experience, the in vivo recombination of mutagenic libraries can confer significant advantages when compared with in vitro recombination protocols, particularly in terms of cloning simplicity and the quality of the libraries generated (Alcalde, 2010). The high level of homologous recombination of *S. cerevisiae* allowed us to repair the mutagenized products within the linear vector in vivo by engineering specifically overlapping regions without altering the ORF. Mutagenic libraries were recombined by in vivo DNA shuffling and/or by in vivo assembly of mutant libraries with different mutational spectra (IvAM) (Okkels, 2004; Zumárraga et al., 2008a). To enhance the number of crossover events among the inserts without compromising the transformation efficiency, several overlapping regions with lower homology to the linear vector were tested. The mutational rate was tuned so that ~1–3 amino acid changes per fusion protein were introduced on average for each cycle of evolution (Tracewell and Arnold, 2009).

Over 50,000 clones were explored in eight rounds of directed evolution and site-directed mutagenesis, culminating in the selection of the ultimate variant, the OB-1 mutant, with a 34,000-fold total activity improvement (TAI) over α-PM1 (the TAI value represents the joint enhancement of specific activity and secretion; Figure 1). Regardless of the enzyme and the attribute subjected to in vitro evolution, it is rare to achieve such a strong improvement. It seems plausible that by jointly evolving the α-factor prepro-leader along with the mature PM1 for secretion in yeast, a synergic effect between both polypeptides has occurred, eventually improving the exportation of α-PM1 in the eukaryotic host. During the artificial evolution pathway (Figure 1), 26 mutants with improvements ranging from 1.3- to 12-fold against the best corresponding parental type were characterized in each cycle and further recombined. In general terms, up to 28 different positions were mutated (nine of them synonymous mutations) throughout the α-PM1 fusion gene (Table S1). From these, nine mutations were found in the α-factor prepro-leader and the remaining 19 in the laccase gene.

The first two rounds of evolution involved error-prone PCR at different mutational rates and with DNA polymerases that had distinct mutational bias (Figure 1; Table S1). To speed up the evolution process, from the second round onward, a protocol was used that combined the construction of mutant libraries from each parental type by in vivo DNA shuffling. This strategy produced complex crossover events for each offspring, along with the introduction of new point mutations (Figure 2). The best variant from the fifth cycle, mutant 7H2, had ~24,300-fold improved activity over α-PM1, with a total laccase activity of 1000 U/L. The preliminary characterization of 7H2 demonstrated

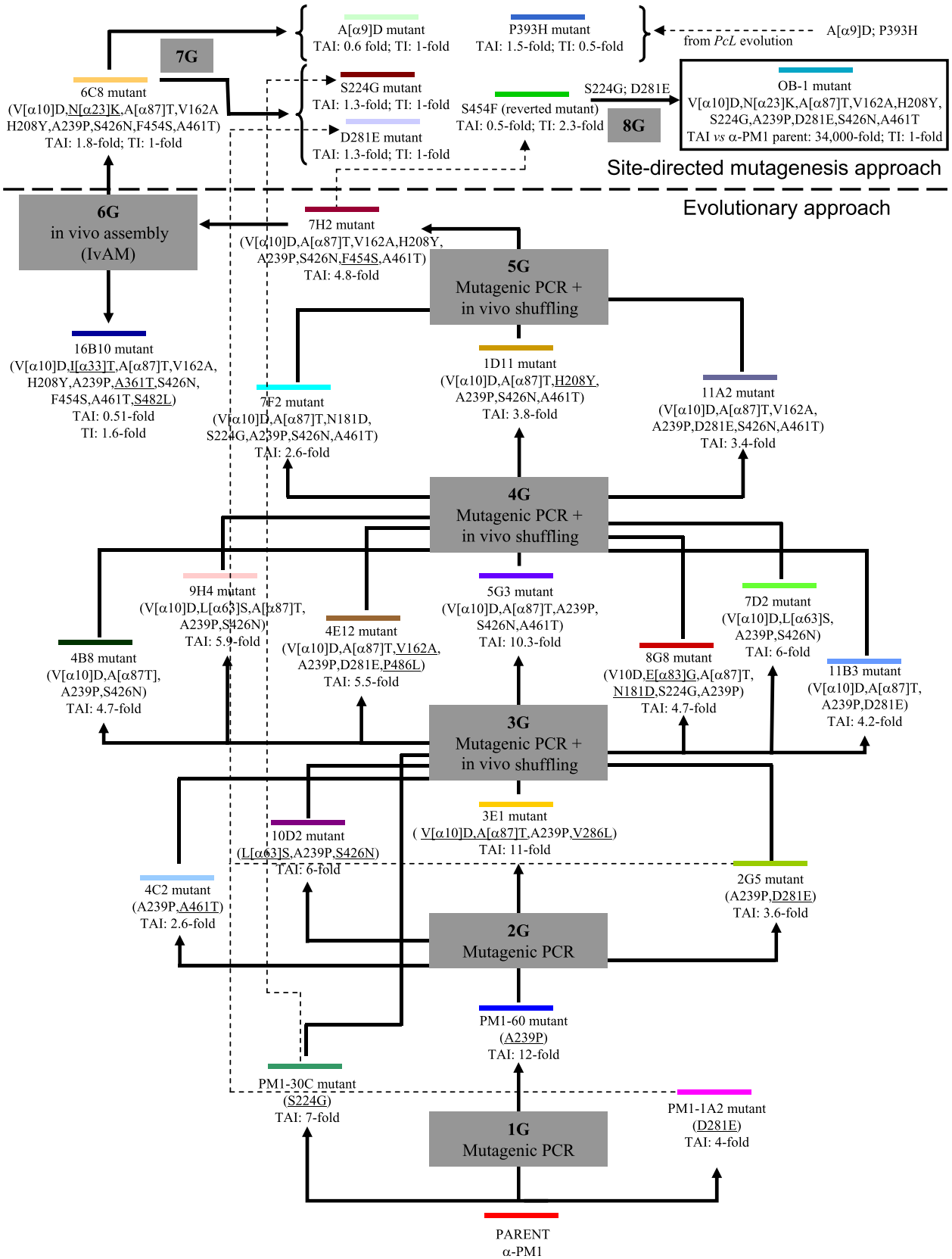
A[α9]D mutant
TAI: 0.6 fold; TI: 1-fold
P393H mutant
TAI: 1.5-fold; TI: 0.5-fold
A[α9]D; P393H
from PcL evolution
7G
6C8 mutant
(V[α10]D,N[α23]K,A[α87]T,V162A
H208Y,A239P,S426N,F454S,A461T)
TAI: 1.8-fold; TI: 1-fold
S224G mutant
TAI: 1.3-fold; TI: 1-fold
D281E mutant
TAI: 1.3-fold; TI: 1-fold
S454F (reverted mutant)
TAI: 0.5-fold; TI: 2.3-fold
S224G; D281E
8G
OB-1 mutant
V[α10]D,N[α23]K,A[α87]T,V162A,H208Y,
S224G,A239P,D281E,S426N,A461T
TAI vs α-PM1 parent: 34,000-fold; TI: 1-fold
Site-directed mutagenesis approach
Evolutionary approach
6G
in vivo assembly
(IvAM)
7H2 mutant
(V[α10]D,A[α87]T,V162A,H208Y,
A239P,S426N,F454S,A461T)
TAI: 4.8-fold
5G
Mutagenic PCR +
in vivo shuffling
16B10 mutant
(V[α10]D,I[α33]T,A[α87]T,V162A,
H208Y,A239P,A361T,S426N,
F454S,A461T,S482L)
TAI: 0.51-fold
TI: 1.6-fold
7F2 mutant
(V[α10]D,A[α87]T,N181D,
S224G,A239P,S426N,A461T)
TAI: 2.6-fold
1D11 mutant
(V[α10]D,A[α87]T,H208Y,
A239P,S426N,A461T)
TAI: 3.8-fold
11A2 mutant
(V[α10]D,A[α87]T,V162A,
A239P,D281E,S426N,A461T)
TAI: 3.4-fold
4G
Mutagenic PCR +
in vivo shuffling
9H4 mutant
(V[α10]D,L[α63]S,A[α87]T,
A239P,S426N)
TAI: 5.9-fold
5G3 mutant
(V[α10]D,A[α87]T,A239P,
S426N,A461T)
TAI: 10.3-fold
7D2 mutant
(V[α10]D,L[α63]S,
A239P,S426N)
TAI: 6-fold
4B8 mutant
(V[α10]D,A[α87T],
A239P,S426N)
TAI: 4.7-fold
4E12 mutant
(V[α10]D,A[α87]T,V162A,
A239P,D281E,P486L)
TAI: 5.5-fold
8G8 mutant
(V10D,E[α83]G,A[α87]T,
N181D,S224G,A239P)
TAI: 4.7-fold
11B3 mutant
(V[α10]D,A[α87]T,
A239P,D281E)
TAI: 4.2-fold
3G
Mutagenic PCR +
in vivo shuffling
3E1 mutant
(V[α10]D,A[α87]T,A239P,V286L)
TAI: 11-fold
10D2 mutant
(L[α63]S,A239P,S426N)
TAI: 6-fold
4C2 mutant
(A239P,A461T)
TAI: 2.6-fold
2G5 mutant
(A239P,D281E)
TAI: 3.6-fold
2G
Mutagenic PCR
PM1-60 mutant
(A239P)
TAI: 12-fold
PM1-30C mutant
(S224G)
TAI: 7-fold
PM1-1A2 mutant
(D281E)
TAI: 4-fold
1G
Mutagenic PCR
PARENT
α-PM1

a strong reduction in its thermostability with a decrease in the T_{50} of ~5°C with respect to its corresponding parental, 1D11 and 11A2 mutants (from 73°C to 68°C; Figure 3B), which was coupled to a significant drop during its long-term storage (losing ~30% of its activity after 14 days at 4°C). The accumulation of beneficial but destabilizing mutations during evolution is a well known phenomenon (Bloom et al., 2006; Bloom and Arnold, 2009; García-Ruiz et al., 2010 and references therein). To overcome this shortcoming and to recover the stability while tolerating the introduction of a new set of beneficial mutations, a thermostability screening assay was incorporated in the sixth round on the basis of the determination of the T_{50} (defined as the temperature at which the enzyme retains 50% of its activity after a 10 min incubation) (García-Ruiz et al., 2010; Bommarius et al., 2006). On this occasion, the library was constructed by IvAM, mixing different mutational profiles and biases (Zumárraga et al., 2008a). The best thermostable variant, 16B10, recovered part of its thermostability with an improvement in its T_{50} of 3°C (Figure 3B), albeit at expense of its activity, which halved from 1000 to 510 U/L (Figure 1; Table S1). On the other hand, the variant with the best activity in this cycle, 6C8, still improved the total activity values to ~2000 U/L while maintaining similar stability to 7H2. At this point, we reached a crossroads where we could either continue evolving thermostability from 16B10 while endangering its activity, or use the 6C8 mutant as the parent and try to resolve the stability issue "rationally." Rather than facing the well known trade-off that usually arises between activity and stability for many single point mutations (Romero and Arnold, 2009), we went back to analyze the unstable 7H2. This mutant came from a crossover event between 1D11 and 11A2, which allowed us to join the V(α10)D, A(α87)T, and V162A mutations in the 11A2 mutant with H208Y, A239P, S426N, and A461T in the 1D11 mutant (Figure 2; Table S1). Moreover, 7H2 incorporated one synonymous mutation plus mutation F454S, generated by random mutagenesis in combination with in vivo DNA shuffling. We mapped this mutation in a 3D-structure model based on the crystal structure of the *Trametes trogii* laccase (97% identity, Matera et al., 2008). Phe454 is located in an alpha helix close to the T1 Cu site, the place where the reducing substrate binds. In fact, Phe454 lies next to one of the coordinating ligands of the T1 Cu, the His455 that seems to be involved in binding the reducing substrate enabling the entrance of electrons to the T1 Cu (Bertrand et al., 2002; Matera et al., 2008). Inspection of the protein model suggests that the F454S mutation allows an additional hydrogen bond to form with Ala161 (Figure 3A). It seems plausible that this new hydrogen bond might provoke the movement of the helicoidal segment where His455 is found, amplifying the distance between the coordinating ligand and the T1 Cu. This effect would increase the catalytic rate, but it would dramatically affect the stability of the variant. Therefore, we decided to reverse the F454S mutation in the 6C8 mutant by site-directed mutagenesis. The resulting S454F reverted variant completely recovered its stability with a T_{50} identical to the parents from the fourth round and beyond (Figure 3C). Notably, while the reverted mutant decreased its activity by half (900 U/L), it displayed a similar activity to that reported for 7H2 and it was again very thermostable. The synergistic effect of recombining 1D11 and 11A2, along with the new beneficial mutation that appeared in 6C8 (N[α23]K) overcame the loss of the beneficial but destabilizing F454S mutation in terms of the overall improvement in activity.

Recovery of Beneficial Mutations

During the engineering of the HRPL in *S. cerevisiae*, some of the mutations discovered in the early stages of evolution that affected activity were eventually discarded by the *S. cerevisiae* recombination apparatus, despite their potential benefits. In the eukaryotic host, the likelihood of a crossover event occurring between two mutations is directly proportional to the number of nucleotides separating those mutations. Thus, it is not surprising that some beneficial mutations were not eventually incorporated in a scaffold that already contained the mutation A239P, such as S224G or D281E (Figure 2). We thought that it would be interesting to rescue these mutations and test them individually in the 6C8 variant. Mutation S224G was the only mutation harbored by the PM1-30C mutant (from the first generation) producing a seven-fold improvement in activity (Figure 1). This variant was again used as a parent in the third round for backcrossing, and S224G was incorporated into the offspring. Unfortunately, as a result of the aforementioned crossover between 1D11 and 11A2 in the fifth round, S224G was finally lost. Likewise, the D281E mutation appeared separately in different points in evolution (in the PM1-1A2 and 2G5 mutants from first and second round of evolution with improvements of 4- and 3.6-fold, respectively). Once again, the recombination event between 1D11 and 11A2 ruled out D281E from the laccase gene. Both these mutations were studied individually by site-directed mutagenesis in the seventh round and, in both cases, the total activity was enhanced without compromising thermostability (Figures 1 and 3C). Accordingly, S224G and D281E were both incorporated into the reverted variant in the last cycle giving rise to the OB-1 mutant.

Mutational Exchange with a Related Evolved HRPL

In a parallel effort, we were also involved in the directed evolution of another HRPL from *Pycnoporus cinnabarinus* (Camarero et al., 2009; unpublished data), which shares 77% identity with the PM1 laccase. Mimicking the same approach as that followed with the PM1 laccase, the native signal sequence of *P. cinnabarinus*

Figure 1. Artificial Evolution Pathway for α-PM1

A combination of evolutionary approaches (random mutagenesis, in vivo DNA shuffling, and IvAM) and rational strategies (site directed mutagenesis for both beneficial mutational recovery and mutational exchange with related evolved HRPL) was used during the evolution of the α-PM1 fusion gene. The new point mutations are underlined. The points of departure for mutations incorporated in the seventh round by site-directed mutagenesis are indicated by the dashed arrows. TAI (total activity improvement): this value indicates the improvement in laccase activity detected in *S. cerevisiae* microcultures for each mutant selected when compared with the best parental type of the corresponding generation. Measurements were made in quintuplet from supernatants of independent cultures grown in 96-well plates, using 3 mM ABTS as the substrate (see the Supplemental Experimental Procedures for further details). The OB-1 mutant had an accumulated TAI value of 34,000-fold that of the original parental α-PM1 type. The breakdown of the TAI into specific activity and level of expression is represented in Table 1. TI: thermostability improvement versus parental type of the corresponding generation. PcL: Laccase from *Pycnoporus cinnabarinus* (see section Mutational Exchange with a Related Evolved HRPL; see also Figures S2 and S3, and Table S1).

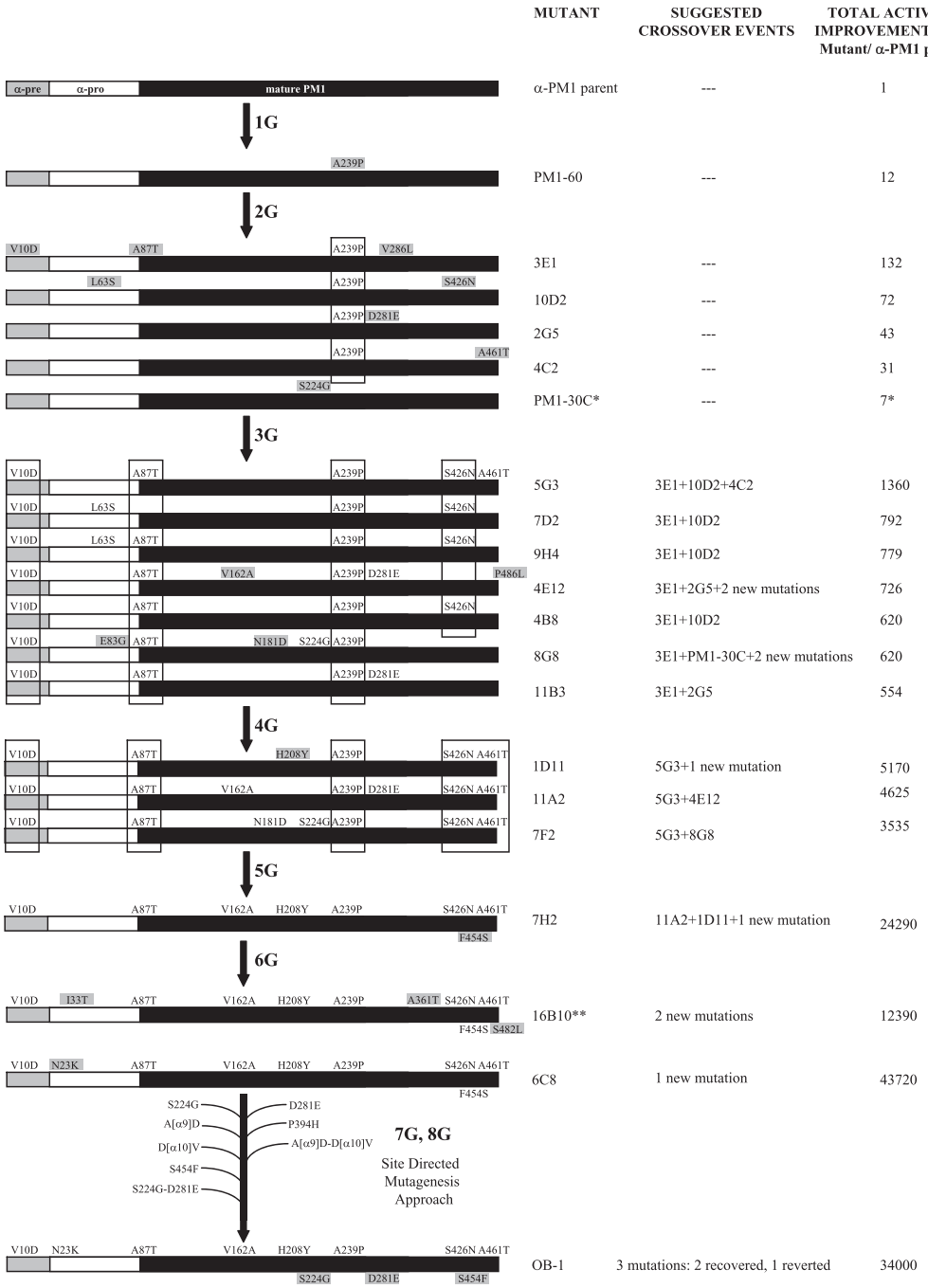

Figure 2. Suggested Crossover Events During the Directed Evolution of α-PM1

The α-factor preleader is represented in gray, the α-factor proleader in white, and the mature PM1 in black. New point mutations are highlighted in gray. With single asterisk is highlighted PM1-30C, the second best mutant from first generation which was recovered for backcrossing in the third round. With double asterisk is highlighted 16B10 mutant, the best thermostability mutant of the sixth round. TAI values are in reference to the original parental α-PM1 expressed in *S. cerevisiae.* See also Tables S1 and S2.

laccase was also replaced by the α-factor prepro-leader, and the corresponding fusion protein was subjected to several rounds of random mutagenesis and recombination (Figure S2). One of the best mutations found during the evolution of *P. cinnabarinus* laccase (P394H) lies in the vicinity of the T1 Cu. The replacement of Pro by His at position 394 promotes a new hydrogen bond with Asn208 that is close to His395, one of the ligands of T1 Cu (Camarero et al., 2009). The sequence alignment of PM1 with *P. cinnabarinus* laccase indicates that P394 belongs to a highly conserved region in HRPLs (Figure S3). Accordingly, the P394H

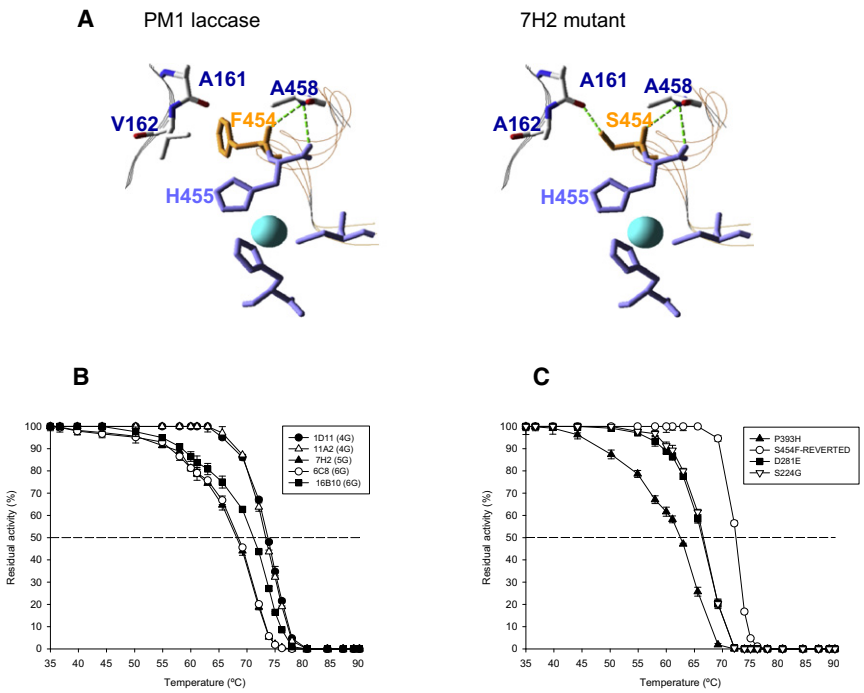

Figure 3. Rational Approach to Thermostability

(A) Detail of a 3D laccase model showing the location of Residue 454 in the vicinity of the T1 Cu site for the parental PM1 and 7H2 mutants. S454 establishes two H-bonds with A458 and after mutation, an additional bond with A161 is formed. Blue sphere, T1 copper.

(B) Thermostability of evolved HRPLs: T_{50} of mutants from fourth, fifth, and sixth generations. Black circles, 1D11 mutant (4^{th} G); white triangles, 11A2 mutant (4^{th} G); black triangles, 7H2 mutant (5^{th} G); white circles, 6C8 mutant (6^{th} G); black squares, 16B10 mutant (6^{th} G). Each point, including the standard deviation, is from three independent experiments.

(C) T_{50} of mutants constructed by site-directed mutagenesis using the 6C8 mutant as the template. Black triangles, P393H mutant; black squares, D281E mutant; white inverted triangle, S224G mutant; white circles, S454F reverted mutant. Each point, including the standard deviation, is from three independent experiments.

mutation (P393H using the PM1 numbering) was introduced into 6C8 during the seventh cycle, improving its activity to ~3000 U/L but with a significant decrease in thermostability (the T_{50} decreased by 2°C) (Figure 3C). We truly do not know whether the loss in thermostability upon mutation was a common side effect in both laccases or if it only occurred in the evolved 6C8. In fact, an analysis of thermostability could not be performed in the *P. cinnabarinus* laccase because P394H was introduced in the first round of evolution, when the expression levels were virtually undetectable (Figure S2). Taking into account that our main goal was to tailor a highly active and stable HRPL, and despite the improvement in activity, P393H was not eventually incorporated into the last variant, the OB-1 mutant.

Directed Evolution of the α-Factor Prepro-Leader

The α-factor prepro-leader encodes an 83–amino acid polypeptide of which the first 19 residues constitute the preleader that direct the nascent polypeptide to the endoplasmic reticulum (ER). Upon extrusion into the ER, the preleader is cleaved by a signal peptidase leaving a proprotein. At this point, N-linked glycosylation of three asparagine residues in the proleader facilitates ER to Golgi transit, and in the Golgi compartment, the proleader may act as chaperone until it is processed by the *KEX1*, *KEX2*, and *STE13* proteases (Romanos et al., 1992; Shuster, 1991). In addition, the proleader is thought to be involved in vacuolar targeting, which is detrimental to heterologous secretion (Rakestraw et al., 2009). Up to eight mutations (three synonymous) were introduced into the α-factor prepro-leader during α-PM1 laboratory evolution, although only V[α10]D, N[α23]K, A[α87]T and the synonymous G[α62]G were conserved in the ultimate OB-1 variant. V[α10]D was located in the hydrophobic domain of the preleader and, interestingly, one of the best mutations found during the evolution of the *P. cinnabarinus* laccase fused with the α-factor prepro-leader was also discovered in this domain (mutation A[α9]D, Figure S2). It has been reported that mutations in the preregion can affect ER targeting and secretion (Romanos et al., 1992). The role of these two consecutive mutations in laccase trafficking was tested in single, double, and reverted mutants constructed in the 6C8 template during the seventh round (Table S2). The experimental data indicated that, individually, A[α9]D and V[α10]D exerted a 2.2-fold improvement in secretion but when they were combined, the hydrophobicity of this domain was drastically diminished. It is well known that most alterations that reduce the translocation efficiency are related with an overall decrease in the hydrophobicity of this domain (Romanos et al., 1992). We assume that the individual changes of charged carboxylic residues at positions 9 or 10 of the α-factor preleader may positively affect the interaction between the signal peptide and the signal recognition particle involved in orienting and inserting the polypeptide laccase chain into the membrane bilayer of the ER (Nothwehr and Gordon, 1990; Boyd and Beckwith, 1990). The mutation N[α23]K was situated at the first of the three sites for Asn-linked glycosylation in the proleader (Romanos et al., 1992). Although it is not absolutely essential for secretion, such glycosylation might facilitate ER to Golgi transport (Rakestraw et al., 2009). However, our results did not support this hypothesis because removal of the glycosylation site in the sixth round (giving rise to 6C8) improved secretion. Finally, the A[α87]T mutation was found in the processing site of *STE13*, a dipeptidyl aminopeptidase that removes the spacer residues (Glu/Asp-Ala)2 at the amino terminus between the α-factor proleader and the mature PM1. After mutation, the spacer residues provide an even more hydrophilic environment at the adjacent *KEX2* cleavage site (Lys-Arg), which might affect the secretion of mature laccase (Brake, 1990).

Table 1. Comparison of the Kinetic Parameters of PM1 Mutants Expressed in *S. cerevisiae* and of the Highly Related *Trametes* C30 and *Trametes trogii* Laccases

HRPL	Generation	Substrate	K_m (mM)	k_{cat} (s^{-1})	k_{cat}/K_m ($mM^{-1}s^{-1}$)	Total activity improvement TAI[c] (fold increase)		Improvement *vs* 3E1 mutant[d]	
						vs α-PM1	*vs* 3E1 mutant	k_{cat}	Expression
3E1 mutant	2	ABTS	0.009 ± 0.002	15.7 ± 0.8	1744	132	1	1	1
		DMP	0.068 ± 0.005	7.7 ± 0.1	113				
		Guaiacol	0.95 ± 0.07	3.31 ± 0.05	3.5				
5G3 mutant	3	ABTS	0.020 ± 0.006	54 ± 5	2700	1360	10	3.4	3
		DMP	0.087 ± 0.009	20.6 ± 0.5	237				
		Guaiacol	2.09 ± 0.08	8.43 ± 0.08	4.0				
1D11 mutant	4	ABTS	0.013 ± 0.002	105 ± 4	8077	5170	39	6.7	6
		DMP	0.106 ± 0.006	40.9 ± 0.6	386				
		Guaiacol	2.10 ± 0.08	18.5 ± 0.2	8.8				
OB-1 mutant	8	ABTS	0.0063 ± 0.0009	200 ± 7	31746	34000	255	12.7	20
		DMP	0.14 ± 0.02	134 ± 5	957				
		Guaiacol	4.6 ± 0.1	90 ± 1	20				
T. trogii LccI[a]	—	ABTS	0.0083 ± 0.0003	98	11807	—	—	—	—
		DMP	0.195 ± 0.0001	51	262				
		Guaiacol	3.073 ± 0.088	6.5	2.1				
T. C30 Lac1[b]	—	ABTS	0.0107	56	5234	—	—	—	—
		DMP	n.r.	n.r.	n.r.				
		Guaiacol	n.r.	n.r.	n.r.				

[a] Data from Colao et al. 2006.
[b] Data from Klonowska et al., 2002.
[c] TAI: total activity improvement with respect to the α-PM1 parental type and the 3E1 mutant from the second generation. The TAI was measured using 3 mM ABTS as the substrate in supernatants of cultures grown in 96-well plates. The numbers are the averages of five measurements.
[d] Dissection of the TAI for activity (K_{cat}) and expression in reference to the 3E1 mutant (second generation). The improvement in expression is defined as the ratio of the total increase in activity and K_{cat} with ABTS as the substrate. n.r., not reported.

Characterization of the OB-1 Mutant

The last mutant obtained, the OB-1 variant, was purified to homogeneity and characterized biochemically (Table 1 and Figure 4; Figure S4). The specific activity of the OB-1 mutant was 400 U/mg and it was secreted with levels of ~8 mg/L. The molecular mass of OB-1 was estimated by MALDI-TOF mass spectrometry as 60,310 Da, 3,690 Da below the molecular weight reported for the native laccase expressed by the basidiomycete PM1 (Coll et al., 1993a) (Figure S4). The molecular mass determined from the amino acid composition of OB-1 was 53,284 Da, and the contribution of glycosylation deduced from the deglycosylation pattern was ~10% (Figure S4). Our results in *S. cerevisiae* from the directed evolution of laccases from *P. cinnabarinus* (PcL) (Camarero et al., 2009 and unpublished data) and *M. thermophila* (MtL) were quite different (Bulter et al., 2003; Zumárraga et al., 2007), and unlike the OB-1 variant, the PcL and MtL mutants were hyperglycosylated with sugar moieties contributing around 50% of their molecular weight. Because complex outer chain carbohydrate addition occurs in the Golgi apparatus, incorporating mannose moieties, hyperglycosylation can be considered to be a consequence of longer residence times in this cellular compartment. We assumed that the evolved mutant is readily secreted by *S. cerevisiae*, whereas other heterologous laccases experience serious difficulties in exiting the Golgi. The pH profiles of relative activities versus phenolic and nonphenolic compounds were not significantly altered during evolution, with OB-1 and the former evolved variants displaying similar optimal pH values (~4.0 and 3.0 for DMP and ABTS, respectively; Figures 4A and 4B). Unfortunately, the very low expression levels of the parental α-PM1 (0.035 ABTS-Units/L) did not enable us to purify it in sufficient quantity to be able to characterize it kinetically and compare it with the evolved mutants. However, the total activity improvements (TAIs) obtained in the evolution process were determined as the improvement in specific activity and expression. To this end, several variants from the second round of evolution onward were produced and characterized kinetically using classic laccase substrates (Table 1). The improvement in activity was not dependent on the substrate, since the catalytic efficiencies were enhanced in each round of evolution regardless of the substrate tested. The last mutant, OB-1, displayed a 13-fold increase in K_{cat} together with 20-fold increase in functional expression when compared to the best variant from the second generation, the 3E1 mutant, which correspondingly had a 132-fold TAI when compared with the original parental type α-PM1. Similarly, the catalytic efficiency of OB-1 was up to six-fold better than that reported for the highly related *Trametes* C30 and *Trametes trogii* laccases, which were 99% and 97% identical to the PM1 laccase, respectively (Klonowska et al., 2002; Colao et al., 2006). Notably, after eight rounds of evolution, the thermostability of OB-1 mutant was 100% conserved, with a T_{50} value of ~73°C. PM1 laccase belongs to the group of HRPLs isolated from the western

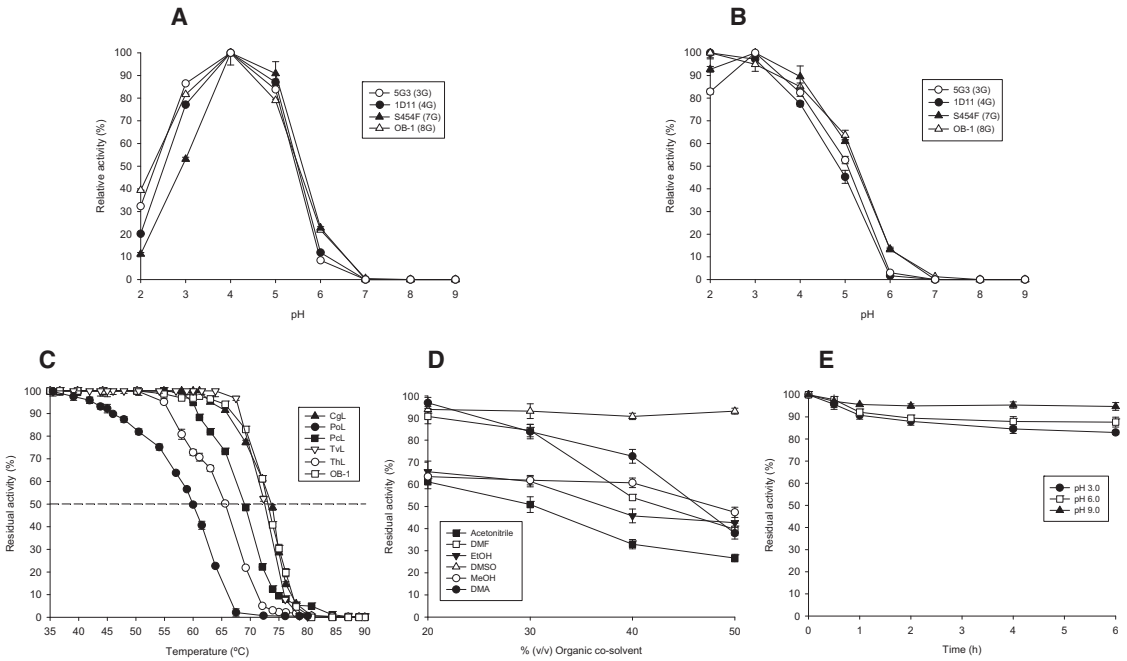

Figure 4. Biochemical Characterization of OB-1 Mutant

(A and B) pH activity profiles of mutant laccases. White circles, 5G3 mutant (3rd G); black circles, 1D11 mutant (4th G); black triangles, S454F mutant (7th G); white triangles, OB-1 mutant (8th G). Activities were measured in 100 mM Britton and Robinson buffer at different pHs with 3 mM DMP (A) or ABTS (B) as the substrates. Laccase activity was normalized to the optimum activity value and each point, including the standard deviation, in three independent experiments.

(C) T_{50} of the OB-1 mutant and other related HRPLs. Black triangle, *Coriolopsis gallica* laccase; black circles, *Pleurotus ostreatus* laccase; black squares, *Pycnoporus cinnabarinus* laccase; white inverted triangles, *Trametes versicolor* laccase; white circles, *Trametes hirsuta* laccase; white squares, the OB-1 mutant. Each point, including the standard deviation, is from three independent experiments.

(D) Stability of OB-1 in the presence of increasing concentrations (v/v) of several organic cosolvents. The experiments were performed in screw-cap vials containing the OB-1 variant in a cosolvent/100 mM Britton and Robison buffer (pH 6.0) mixture. After 4 hr, aliquots were removed and assayed for activity with 3 mM ABTS in 100 mM sodium acetate buffer (pH 4.0). Black squares, acetonitrile; black inverted triangles, ethanol; white squares, dimethyl formamide; white circles; methanol; black circles, dimethyl acetamide; white triangles, dimethyl sulfoxide. Residual activity was expressed as the percentage of the original activity at the corresponding concentration of organic cosolvent. Each point, including the standard deviation, is from three independent experiments.

(E) The pH stability of the OB-1 mutant at pH 3.0, 6.0, and 9.0. Enzyme samples were incubated in 10 mM Britton and Robinson buffer at different pH values, and residual activity was measured in 3 mM ABTS in 100 mM sodium acetate buffer (pH 4.0). Black circles, pH 3.0; white squares, pH 6.0; black triangles, pH 9.0. Each point, including the standard deviation, comes from three independent experiments. See also Figure S4.

Mediterranean area, together with *T. trogii* laccase, *Trametes* C30 laccase, or *Coriolopsis gallica* laccase. All these HRPLs share a high degree of sequence identity (above 97%) and similar biochemical features, including in all cases strong thermostability (Colao et al., 2003; Hilden et al., 2009). To additionally evaluate the thermostability of our evolved laccase, it was compared with a battery of HRPLs from different sources (Figure 4C). The T_{50} of OB-1 mutant was higher than that of HRPLs from *Trametes hirsuta*, *P. cinnabarinus*, or *Pleurotus ostreatus* and similar to the T_{50} of laccases from *Coriolopsis gallica* and *T. versicolor*. The stability of OB-1 was further evaluated in the presence of high concentrations of organic cosolvents with different polarities and chemical nature, (Figure 4D). As expected from a highly thermostable enzyme (Zumárraga et al., 2007), the evolved PM1 laccase was quite tolerant to the presence of cosolvents (retaining 30%–90% of its activity after 4 hr at solvent concentrations as high as 50% (v/v)). The stability of the evolved laccase at different pHs was also evaluated, keeping ~90% of its activity in the pH range of 3–9 after 4 hr of incubation (Figure 4E).

The ultimate OB-1 variant accumulated 15 mutations: five in the α-factor prepro-leader (two synonymous) and ten in the mature protein (three synonymous). Three of the five synonymous mutations favored codon usage (Table S1), which may be a factor that potentially favors the yield of secretion by affecting the elongation rate (Romanos et al., 1992). In general terms, strongly expressed genes show a bias toward a specific subset of codons (Dix and Thompson, 1989) and, thus, codon optimization may be important for the expression of laccases in yeast. Hence, the protein abundance may be modulated by the differential usage of synonymous codons, which is closed related to the levels of the corresponding tRNAs in the eukaryotic apparatus. Very recently, it was reported that translation efficiency can be also regulated by the folding energy of the mRNA transcript, which may affect ribosome binding and the translation initiation (Tuller et al., 2010).

Beneficial mutations in the mature laccase basically mapped to rather accessible residues, some located far from the catalytic coppers, whereas others were in the vicinity of the catalytic sites (Figure 5 and Table 2, and Figure S5, summarize the features of these changes in the laccase structure). In particular, the V162A, S426N and A461T mutations are in the T1 Cu neighborhood. Val162 is one of the hydrophobic residues in the loop

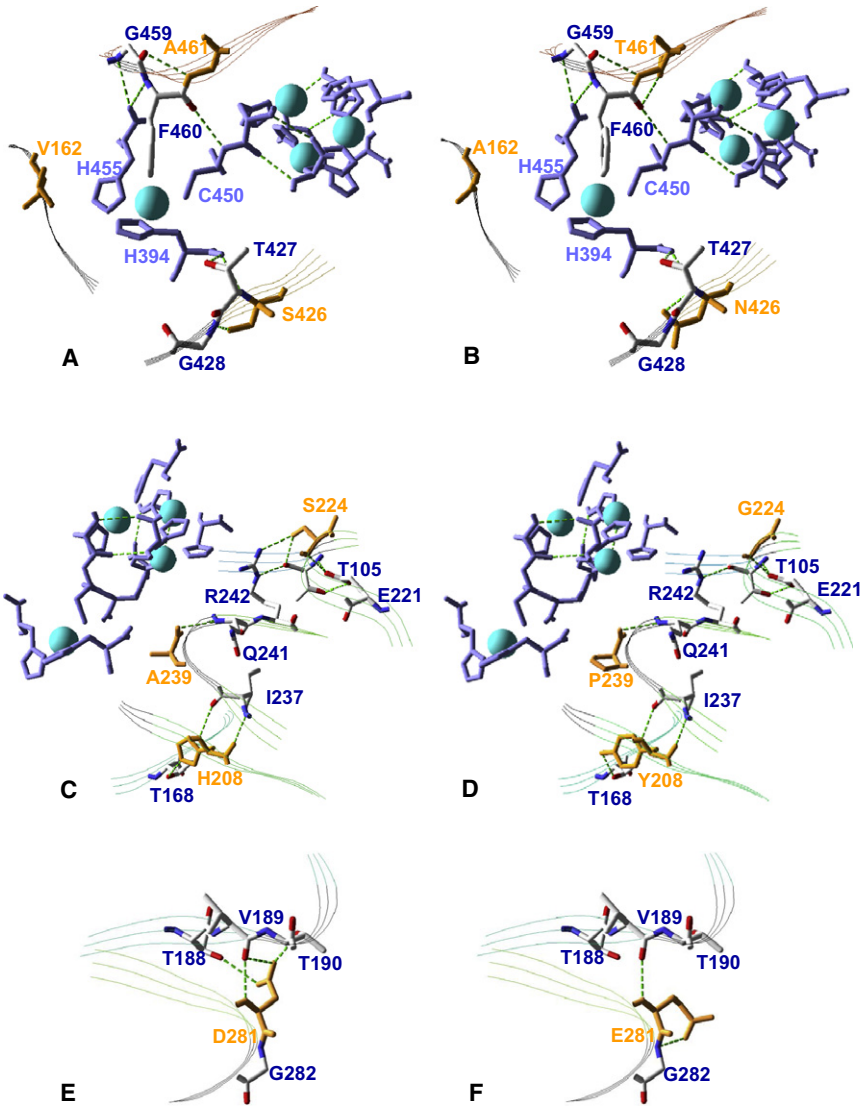

Figure 5. Mutations in Evolved Laccase

Details of the seven mutations (in orange) in the OB-1 variant (B, D, and F) compared with the corresponding residues in the native PM1 laccase (A, C, and E). Ligands of T1 Cu and the T2/T3 trinuclear Cu cluster are shown in light blue. Blue spheres represent Cu atoms H-bonds involving the mutated residues (before and after mutation) are shown as green dashes. See also Figure S5.

that delimits the cavity of the substrate pocket at the T1 site (Bertrand et al., 2002). The change from Val to Ala at this position represents the substitution of a hydrophobic residue by another somewhat smaller hydrophobic one, which may favor substrate binding (Figures 5A and 5B). Ser426 is H-bonded to Gly428 but after mutation the H-bond no longer exists. The inspection of the protein model suggests that the resulting Asn426 may establish a new H-bond with the adjacent Thr427 residue. In turn, the latter is double bonded to the T1 Cu ligand His394, such that this change might affect the position of His394 relative to the T1 site (Figures 5A and 5B). Ala461 is adjacent to Phe460 (the position for the fourth axial ligand in plant and bacterial laccases) (Alcalde, 2007)), the latter establishing hydrogen bonds with the T1 Cu ligands, His455 and Cys450. The A461T mutation seems to render a new H-bond with Phe460, which might change the local geometry of the T1 site (Xu et al., 1998) (Figures 5A and 5B).

Most of the remaining beneficial mutations (H208Y, S224G, A239P, and D281E) were mapped far from the catalytic coppers, appearing in coils or secondary motifs whose role in the laccase function remains uncertain (Table 2 and Figures 5C–5F). It is highly unlikely that such mutations could have been anticipated by rational design; however, the use of directed evolution has unmasked a functional relevance to these previously unknown regions of laccases. For instance, Asp281 is located in a distal loop of the D2 domain that is almost completely exposed at the protein surface (at ~40 Å from the T1 Cu site). Our protein model suggests that the replacement of Asp by Glu at position 281 breaks two H-bonds with Thr188 and Thr190 in a neighboring loop and may produce a new H-bond with Gly282 of the same motif, which might increase the flexibility of this zone (Figures 5E and 5F). That the above-mentioned mutations improve folding and maturation in *S. cerevisiae* cannot be ruled out, in addition to their possible contribution to the final robustness of the protein.

SIGNIFICANCE

HRPLs are a clear example of generalist biocatalysts that make a virtue of their substrate promiscuity. Fueled by molecular oxygen, they transform hundreds of substrates of different nature and complexity, ranging from xenobiotics (e.g., pesticides, industrial dyes, and PAHs) to biopolymers (lignin and starch). Hence, HRPLs have potential applications in bioremediation, finishing of textiles, pulp-paper biobleaching, biofuels, organic synthesis, and many other processes (Xu, 2005; Kunamneni et al., 2008a; Widsten and Kandelbauer, 2008, Bragd et al., 2004). In addition, HRPLs are among the few enzymes capable of accepting electrons in a direct manner from a cathodic compartment, thus being essential for bioelectrochemists in the engineering of nanobiodevices and generating special interest for the engineering of 3D-bionanosensors and biofuel cells (Shleev et al., 2005b). Unfortunately, their practical design by directed evolution has hitherto been hampered by the lack of appropriate approaches to circumvent the complex problems of their functional expression (Roodveldt et al., 2005). Indeed, there are only a few preliminary studies along these lines because of their poor exocytosys by yeast (Festa

Table 2. Mutations in Mature OB-1 Variant

Mutation	Domain	Secondary structure motif	Relative Position	Distance to the T1 Site (Å)	Distance to the T2/T3 (Å)	Interactions by hydrogen bonds with surrounding residues[a]	
						Before mutation	After mutation
V162A	D2	Coil	Surface	9.62	21.29	—	—
H208Y	D2	Beta sheet	Near Asp206 (that binds phenols in Cu T1 site)	14.74	19.33	I237, T168	I237, T168
S224G	D3	Coil	Surface	21.22	9.96	T105, E221, R242	E221
A239P	D2	Coil	Surface	8.57	11.65	Q241	Q241
D281E	D2	Coil	Surface	39.95	35.33	T188, V189, T190	V189, **G282**
S426N	D3	Beta sheet	Surface. At the vicinity of Cu T1, beside T427 (bonded to H394).	8.23	16.40	G428	**T427**
A461T	D3	Beta sheet	Vicinity Cu T1, beside F460 (position of 4th axial ligand).	8.86	10.93	G459	G459, **F460**

[a] Underlined, interrupted bonds after mutation; in bold, new formed bonds after mutation.

et al., 2008; Cusano et al., 2009; Miele et al., 2010). Our tailor–made HRPL is readily exportable in soluble, active, and stable forms, opening a new array of possibilities for further protein engineering. The meticulous experimental design employed, involving directed evolution and site-directed mutagenesis, has been crucial to tailor a highly active and thermostable biocatalyst that can now be adapted to face new challenges. Likewise, the joint evolution of a "foreign" HRPL gene with the α-factor prepro-leader provides a suitable means to improve these capacities from undetectable levels of expression. This approach could now be translated to other related HRPLs, supporting the general idea of using the directed evolution of the α-factor prepro-leader as a common scaffold for the expression of different protein systems (Rakestraw et al., 2009).

EXPERIMENTAL PROCEDURES

Laboratory Evolution: General Aspects

The original parental type α-PM1 fusion gene was constructed as described in the Supplemental Experimental Procedures. For each generation, PCR fragments were cleaned, concentrated, and loaded onto a low-melting-point preparative agarose gel, then purified using the Zymoclean gel DNA recovery kit (Zymo Research). PCR products were cloned under the control of the Gal 1 promoter of the pJRoC30 expression shuttle vector, replacing the native gene in pJRoC30. To remove the native gene, the pJRoC30 plasmid was linearized with *Xho*I and *BamH*I, and the linear plasmid was concentrated and purified as described above for the PCR fragments.

First Generation

Three independent libraries were prepared with distinct DNA-polymerases and under different mutational rates. The first mutagenic library (~15,000 mutants) was constructed with the Genemorph I kit (Stratagene) adjusting the mutation rate to 1.1–3.5 mutations per kb. The second and third mutagenic libraries (~15000 mutants each), were constructed with the Genemorph II kit (Stratagene) adjusting the mutation rate to 0–4.5 and 4.5–9 mutations per kb, respectively. Error-prone PCR was performed on a gradient thermocycler (Mycycler, BioRad) using the following parameters: 95°C for 2 min (1 cycle); 94°C for 0.45 min, 53°C for 0.45 min, and 74°C for 3 min (28 cycles); and 74°C for 10 min (1 cycle). The primers used for amplification were: RMLN sense (5′-CCTCTATACTTTAACGTCAAGG-3′, which binds to bp 160–180 of pJRoC30-αPM1) and RMLC antisense (5′-GGGAGGGCGTGAATGTAAGC-3′, which binds to bp 2028–2048 of pJRoC30-αPM1). To promote in vivo ligation, overhangs of 40 and 66 bp homologous to the linear vector were designed. The PCR products (400 ng) were mixed with the linearized vector (100 ng) and transformed into competent cells using the yeast transformation kit (Sigma). Transformed cells were plated in SC drop-out plates and incubated for 3 days at 30°C. Colonies containing the whole autonomously replicating vector were picked and subjected to the screening assays, as well as to additional rescreenings as described in the Supplemental Experimental Procedures. From the first to the fifth round of evolution, the libraries were explored for improvements in activity and from the sixth round onward, a thermostability assay was incorporated.

Second Generation

The second round was performed by mutagenic PCR construction, with Mutazyme I DNA polymerase and using the PM1-60 mutant as the parental type. The mutational rate was adjusted to 2.1–3.5 mutations per kb and the mutagenic library (~1000 mutants) was prepared as described above for the first round.

Third Generation

The best variants from the second round (3E1, 10D2, 2G5, and 4C2) were submitted to Taq/$MnCl_2$ amplification and recombined by in vivo DNA shuffling (~1000 clones). The PM1-30C mutant from the first round was also included as a parental type for backcrossing. The Taq/$MnCl_2$ amplifications were prepared in a final volume of 50 μl containing 90 nM RMLN, 90 nM RMLC, 0.1 ng/μL mutant template, 0.3 mM dNTPs (0.075 mM each), 3% DMSO, 1.5 mM $MgCl_2$, and 0.05 U/μL Taq polymerase. Different concentrations of $MnCl_2$ were tested to estimate the appropriate mutation rate before adopting 0.01 mM as the final concentration, and PCR was performed as in the former generations. Several overlapping areas, ranging from 5 to 70 bp in size, were designed to enhance the number of crossover events without compromising the transformation efficiency. Mutated PCR products were mixed in equimolar amounts and transformed along with the linearized vector into yeast (ratio PCR products:vector, 4:1).

Fourth Generation

The best variants of the third round (5G3, 7D2, 9H4, 4E12, 4B8, 8G8, and 11B3) were submitted to Taq/$MnCl_2$ amplification and recombined by in vivo DNA shuffling (~1,000 clones), as described for the third generation.

Fifth Generation

The best variants of the fourth round (1D11, 11A2, and 7F2) were subjected to Taq/$MnCl_2$ amplification and recombined by in vivo DNA shuffling (~1000 clones) as described for the fourth generation.

Sixth Generation

A library of ~1300 clones was built by in vivo assembly of mutant libraries constructed with different mutational spectra (IvAM) (Zumárraga et al., 2008a). The 7H2 mutant was used as the parental type, and Taq/$MnCl_2$ and Mutazyme libraries were mixed in equimolar amounts, and transformed into competent *S. cerevisiae* cells along with the linearized vector as described above (ratio library:vector, 8:1). A thermostability screening assay was incorporated from this generation onward (see below).

Site-Directed Mutagenesis

The seventh and eight generations were produced by site-directed mutagenesis by using In Vivo Overlap Extension (IVOE) (Alcalde, 2010) (details in Supplemental Experimental Procedures).

High-Throughput Screening

Activity and thermostability screening assays were performed in solid and liquid format (in 96-well plates) as indicated the Supplemental Experimental Procedures. Selected mutants were produced and purified as described in the Supplemental Experimental Procedures.

SUPPLEMENTAL INFORMATION

Supplemental Information includes two tables, five figures, and Supplemental Experimental Procedures and can be found with this article online at doi:10.1016/j.chembiol.2010.07.010.

ACKNOWLEDGMENTS

We are truly grateful to R. Santamaría from Salamanca University for donating the native PM1 laccase gene and Francisco J. Plou for assistance with the HPLC purification. This study is based upon work funded by EU Projects (NMP4-SL-2009-229255, NMP2-CT-2006-026456, COST Action CM0701) and National projects (CTQ2005-08925-CO2-02, BIO2010-19697 and CCG08-CSIC/PPQ-3706). We also thank NeuronBiopharma for financial support through Research Contracts 020401070029 (Profit Program) and 020401070004 (Idea Program). D.M. is grateful to the CSIC for a JAE fellowship.

Received: April 14, 2010
Revised: July 9, 2010
Accepted: July 12, 2010
Published: September 23, 2010

REFERENCES

Alcalde, M., Ferrer, M., Plou, F.J., and Ballesteros, M. (2006a). Environmental biocatalysis: from remediation with enzymes to novel green processes. Trends Biotechnol. *24*, 281–287.

Alcalde, M., Zumárraga, M., Polaina, J., Ballesteros, A., and Plou, F.J. (2006b). Combinatorial saturation mutagenesis by in vivo overlap extension for the engineering of fungal laccases. Comb. Chem. High Throughpu Screen *9*, 719–727.

Alcalde, M. (2007). Laccase: biological functions, molecular structure and industrial applications. In Industrial enzymes: structure, functions and applications, J. Polaina and A.P. MacCabe, eds. (Dordrecht, The Netherlands: Springer), pp. 459–474.

Alcalde, M. (2010). Mutagenesis protocols in *Saccharomyces cerevisiae* by in vivo overlap extension. In In vitro mutagenesis protocols, 3rd ed. Methods in Molecular Biology, 634. J. Braman, ed. (Totowa, NJ: Springer-Humana Press), pp. 3–15 .

Bertrand, T., Jolivalt, C., Briozzo, P., Caminade, E., Joly, N., Madzak, C., and Mougin, C. (2002). Crystal structure of a four-copper laccase complexed with an arylamine: insights into substrate recognition and correlation with kinetics. Biochemistry *41*, 7325–7333.

Bloom, J.D., and Arnold, F.H. (2009). In the light of directed evolution: pathways of adaptive protein evolution. Proc. Natl. Acad. Sci. USA *106*, 9995–10000.

Bloom, J.D., Labthavikul, S.T., Otey, C.R., and Arnold, F.H. (2006). Protein stability promotes evolvability. Proc. Natl. Acad. Sci. USA *103*, 5869–5874.

Bommarius, A.S., Broering, J.M., Chaparro-Riggers, J.F., and Polizzi, K.M. (2006). High-throughput screening for enhanced protein stability. Curr. Opin. Biotechnol. *17*, 606–610.

Boyd, D., and Beckwith, J. (1990). The role of charged amino acids in the localization of secreted and membrane proteins. Cell *62*, 1031–1033.

Bragd, P.L., van Bekkum, H., and Besemer, A.C. (2004). TEMPO-mediated oxidation of polysaccharides: surver of methods and applications. Top. Catal. *27*, 49–66.

Brake, A.J. (1990). α-factor leader-directed secretion of heterologous proteins from yeast. Methods Enzymol. *185*, 408–421.

Bulter, T., Alcalde, M., Sieber, V., Meinhold, P., Schlachtbauer, C., and Arnold, F.H. (2003). Functional expression of a fungal laccase in *Saccharomyces cerevisiae* by directed evolution. Appl. Environ. Microbiol. *69*, 987–995.

Call, H.P., and Mucke, I. (1997). History, overview and applications of mediated lignolytic systems, especially laccase-mediator-systems (Lignozym(R)-process). J. Biotechnol. *53*, 163–202.

Camarero, S., Cañas, A., Martínez, M.J., Martínez, A.T., Ballesteros, A., Plou, F.J., Record, E., Asther, M., and Alcalde, M. (2009). High redox potential laccases engineered by directed evolution. Patent PCT/ES2009/070516.

Cañas, Al., and Camarero, S. (2010). Laccases and their natural mediators: biotechnological tools for sustainable eco-friendly processes. Biotechnol. Adv. [epub ahead of print] 10.1016/j.biotechadv.2010.05.002.

Cherry, J.R., Lamsa, M.H., Schneider, P., Vind, J., Svendsen, A., Jones, A., and Pedersen, A.H. (1999). Directed Evolution of a fungal peroxidase. Nat. Biotechnol. *17*, 379–384.

Colao, M.C., Garzillo, A.M., Buonocore, V., Schiesser, A., and Ruzzi, M. (2003). Primary structure and transcription analysis of a laccase-encoding gene from the basidiomycete *Trametes trogii*. Appl. Microbiol. Biotechnol. *63*, 153–158.

Colao, M.C., Lupino, S., Garzillo, A.M., Buonocore, V., and Ruzzi, M. (2006). Heterologous expression of lccl gene from *Trametes trogii* in Pichia pastoris and characterization of the recombinant enzyme. Microb. Cell Fact. *5*, 31.

Coll, P.M., Fernándea-Abalos, J.M., Villanueva, J.R., Santamaria, R., and Pérez, P. (1993a). Purification and characterization of a phenoloxidase (laccase) from the lignin-degrading basidiomycete PM1 (cect-2971). Appl. Environ. Microbiol. *59*, 2607–2613.

Coll, P.M., Tabernero, C., Santamaria, R., and Perez, P. (1993b). Characterization and structural-analysis of the laccase-i gene from the newly isolated ligninolytic basidiomycete PM1 (cect 2971). Appl. Environ. Microbiol. *59*, 4129–4135.

Cusano, A.M., Mekmouche, Y., Meglecz, E., and Tron, T. (2009). Plasticity of laccase generated by homeologous recombination in yeast. FEBS J. *276*, 5471–5480.

Dix, D.B., and Thompson, R.C. (1989). Codon choice and gene expression: synonymous codons differ in translational accuracy. Proc. Natl. Acad. Sci. USA *86*, 6888–6892.

Festa, G., Autore, F., Fraternali, F., Giardina, P., and Sannia, G. (2008). Development of new laccases by directed evolution: functional and computational analyses. Proteins *72*, 25–34.

García-Ruiz, E., Maté, D., Ballesteros, A., Martínez, A.T., and Alcalde, M. (2010). Evolving thermostability in mutant libraries of ligninolytic oxidoreductases expressed in yeast. Microb. Cell Fact. *9*, 17.

Gianfreda, L., Xu, F., and Bollag, J. (1999). Laccases: a useful group of oxidoreductive enzymes. Bioremediat. J. *3*, 1–25.

Giardina, P., Faraco, V., Pezzella, C., Piscitelli, A., Vanhulle, S., and Sannia, G. (2010). Laccases: a never-ending story. Cell. Mol. Life Sci. *67*, 369–385.

Hilden, K., Hakala, T.K., and Lundell, T. (2009). Thermotolerant and thermostable laccases. Biotechnol. Lett. *31*, 1117–1128.

Klonowska, A., Gaudin, C., Fournel, A., Asso, M., Le Petit, J., Giorgi, M., and Tron, T. (2002). Characterization of a low redox potential laccase from the basidiomycete C30. Eur. J. Biochem. *269*, 6119–6125.

 ©2010 Elsevier Ltd All rights reserved

Kunamneni, A., Camarero, S., García, C., Plou, F.J., Ballesteros, A., and Alcalde, M. (2008a). Engineering and applications of fungal laccases for organic synthesis. Microb. Cell Fact. *7*, 32.

Kunamneni, A., Plou, F.J., Ballesteros, A., and Alcalde, M. (2008b). Laccase and their applications: a patent review. Recent Pat. Biotechnol. *2*, 10–24.

Matera, I., Gullotto, A., Tilli, S., Ferraroni, M., Scozzafava, A., and Briganti, F. (2008). Crystal structure of the blue multicopper oxidase from the white-rot fungus *Trametes trogii* complexed with p-toluate. Inorg. Chim. Acta *361*, 4129–4137.

Miele, A., Giardina, P., Sannia, G., and Faraco, V. (2010). Random mutants of a *Pleurotus ostreatus* laccase as new biocatalysts for industrial effluents bioremediation. J. Appl. Microbiol. *108*, 998–1006.

Nothwehr, S.F., and Gordon, J.I. (1990). Targeting of proteins into the eukaryotic secretory pathway: signal peptide structure/function relationship. Bioessays *12*, 479–484.

Okkels, J.S. (2004). In vivo gene shuffling in yeast: a fast and easy method for directed evolution of enzymes. In Enzyme functionality: design, engineering, and screening, A. Svendsen, ed. (New York: Marcel Dekker, Inc.), pp. 413–424.

Rakestraw, J.A., Sazinsky, S.L., Piatesi, A., Antipov, E., and Wittrup, K.D. (2009). Directed evolution of a secretory leader for the improved expression of heterologous proteins and full-length antibodies in *Saccharomyces cerevisiae*. Biotechnol. Bioeng. *103*, 1192–1201.

Riva, S. (2006). Laccase: blue enzymes for green chemistry. Trends Biotechnol. *24*, 219–226.

Rodgers, C.J., Blandford, C.F., Giddens, S.R., Skamnioti, P., Armstrong, F.A., and Gurr, S.J. (2010). Designer laccases: a vogue for high-potential fungal enzymes? Trends Biotechnol. *28*, 63–72.

Romanos, M.A., Scorer, C.A., and Clare, J.J. (1992). Foreign gene expression in yeast: a review. Yeast *8*, 423–488.

Romero, P.A., and Arnold, F.H. (2009). Exploring protein fitness landscapes by directed evolution. Nat. Rev. Mol. Cell Biol. *10*, 866–876.

Roodveldt, C., Aharoni, A., and Tawfik, D.S. (2005). Directed evolution of proteins for heterologous expression. Curr. Opin. Struct. Biol. *15*, 50–56.

Shleev, S., Jarosz-Wilkolazka, A., Khalunina, A.S., Morozova, O., Yaropolov, A., Ruzgas, T., and Gorton, L. (2005a). Direct electron transfer reactions of laccases from different origins on carbon electrodes. Bioelectrochemistry *67*, 115–124.

Shleev, S., Tkac, J., Christenson, A., Ruzgas, T., Yaropolov, A.I., Whittaker, J.W., and Gorton, L. (2005b). Direct electron transfer between copper-containing proteins and electrodes. Biosens. Bioelectron. *20*, 2517–2554.

Shuster, J.R. (1991). Gene expression in yeast: protein secretion. Curr. Opin. Biotechnol. *2*, 685–690.

Solomon, E.I., Sundaram, U.M., and Machonkin, T.E. (1996). Multicopper oxidases and oxygenases. Chem. Rev. *96*, 2563–2605.

Tracewell, C.A., and Arnold, F.H. (2009). Directed enzyme evolution: climbing fitness peaks one amino acid at a time. Curr. Opin. Chem. Biol. *13*, 3–9.

Tuller, T., Waldman, Y.Y., Kupiec, M., and Ruppin, E. (2010). Translation efficiency is determined by both codon bias and folding energy. Proc. Natl. Acad. Sci. USA *107*, 3645–3650.

Widsten, P., and Kandelbauer, A. (2008). Laccase applications in the forest products industry: a review. Enzyme Microb. Technol. *42*, 293–307.

Xu, F. (2005). Applications of oxidoreductases: recent progress. Ind. Biotechnol. (New Rochelle N.Y.) *1*, 38–50.

Xu, F., Berka, R.M., Wahleithner, J.A., Nelson, B.A., Shuster, J.R., Brown, S.H., Palmer, A.E., and Solomon, E.I. (1998). Site-directed mutations in fungal laccase: effect on redox potential, activity and pH profile. Biochem. J. *334*, 63–70.

Zumárraga, M., Bulter, T., Shleev, S., Polaina, J., Martínez-Arias, A., Plou, F.J., Ballesteros, A., and Alcalde, M. (2007). In vitro evolution of a fungal laccase in high concentrations of organic cosolvents. Chem. Biol. *14*, 1052–1064.

Zumárraga, M., Camarero, S., Shleev, S., Martinez-Arias, A., Ballesteros, A., Plou, F.J., and Alcalde, M. (2008a). Altering the laccase functionality by in vivo assembly of mutant libraries with different mutational spectra. Proteins *71*, 250–260.

Zumárraga, M., Vaz Domínguez, C., Camarero, S., Shleev, S., Polaina, J., Martínez-Arias, A., Ferrer, M., De Lacey, A.L., Fernández, V.M., Ballesteros, A., Plou, F.J., and Alcalde, M. (2008b). Combinatorial saturation mutagenesis of the *Myceliophthora thermophila* laccase T2 mutant: the connection between the C-terminal plug and the conserved 509VSG511 tripeptide. Comb. Chem. High Throughput Screen *11*, 807–816.